Atmospheric
Chemistry
and Physics
Discussions

Open Access

Quantifying primary and secondary humic-like substances in urban aerosol based on emission source characterization and a source-oriented air quality model

Xinghua Li[1], Junzan Han[1], Philip K. Hopke[2], Jingnan Hu[3], Qi Shu[1], Qing Chang[1], Qi Ying[4]

[1]School of Space and Environment, Beihang University, Beijing, 100191, China

[2]Center for Air Resources Engineering and Science, Clarkson University, Potsdam, NY USA.

[3]State Environmental Protection Key Laboratory of Vehicle Emission Control and Simulation, Chinese Research Academy of Environmental Sciences, Beijing 100012, China

[4]Zachry Department of Civil Engineering, Texas A&M University, College Station, TX 77843, USA

Correspondence to: Xinghua Li (lixinghua@buaa.edu.cn); Qi Ying (qying@civil.tamu.edu)

Abstract: Humic-like substances (HULIS) are a mixture of high molecular weight, water-soluble organic compounds that are widely distributed in atmospheric aerosol. Their sources are rarely studied quantitatively. Biomass burning is generally accepted as a major primary source of ambient humic-like substances (HULIS) with additional secondary material formed in the atmosphere. However, the present study provides direct evidence that residential coal burning is also a significant source of ambient HULIS, especially in the heating season in northern China based on source measurements, ambient sampling and analysis, and apportionment with source-oriented CMAQ modeling. Emissions tests show that residential coal combustion produces 5 to 24% of the emitted organic carbon (OC) as HULIS carbon (HULISc). Estimation of primary emissions of HULIS in Beijing indicated that residential biofuel and coal burning contribute about 70% and 25% of annual primary HULIS, respectively. Vehicle exhaust, industry, and power plants contributions are negligible. Average concentration of ambient HULIS was 7.5 μg/m^3 in atmospheric PM$_{2.5}$ in urban Beijing and HULIS exhibited obvious seasonal variations with the highest concentrations in winter. HULISc account for 7.2% of PM2.5 mass, 24.5% of OC, and 59.5% of WSOC, respectively. HULIS are found to correlate well with K$^+$, Cl$^-$, sulfate, and secondary organic aerosol suggesting its sources include biomass burning, coal combustion and secondary aerosol formation. Source apportionment based on CMAQ modeling shows residential biofuel and coal burning, secondary formation are important annual sources of ambient HULIS, contributing 57.5%, 12.3%, and 25.8%, respectively.

1 Introduction

28

29 Humic-like substances (HULIS) are a mixture of higher molecular weight organic compounds that resemble terrestrial

30 and aquatic humic and fulvic acids with similar structures and properties (Graber and Rudich, 2006). HULIS are widely

31 distributed in the atmospheric aerosol, rain, and cloud and fog droplets and account for a significant proportion of the

32 organic carbon and water-soluble organic carbon (WSOC). For example, Zheng et al. (2013) reported that 9% to 72% of

33 WSOC is HULIS. Because of their water-soluble and strong surface-active properties, HULIS may play an important

34 role in the formation of clouds as condensation nuclei, ice nuclei and through aerosol hygroscopic growth (Dinar et al.,

35 2006; Wang and Knopf, 2011; Gysel et al., 2004). Due to their strong light absorption in the UV range, HULIS can play

36 an active role as brown carbon in the radiative transfer and photochemical processes (Hoffer et al., 2006). HULIS

37 deposition can also lead to a decrease in the albedo of ice and snow surfaces (Beine et al., 2011; France et al., 2011;

38 France et al., 2012). Owing to their redox-active characteristics, HULIS was also suggested to induce adverse health

39 effect (Lin and Yu, 2011; Ghio et al., 1996; Verma et al., 2012).

40 In recent years, studies focusing on the spatial and temporal variations, sources, and formation of HULIS have been

41 reported. A summary of these studies is provided in Table S1. Previous studies have identified primary emission and

42 atmospheric secondary formation as the important sources of HULIS. Among the primary emission sources, biomass

43 burning is generally accepted as a major source of HULIS, with the evidence from ambient and source sampling as well

44 as source apportionment studies (Lin et al., 2010a, b; Kuang et al., 2015; Park and Yu, 2016; Schmidl et al., 2008a, b;

45 Goncalves et al., 2010). Recently, residential coal burning was suggested as an important primary HULIS source during

46 winter (Tan et al., 2016; Voliotis et al., 2017). However, direct evidence of HULIS emission from coal combustion is

47 limited. Only one study on HULIS emitted from residential coal combustion was reported and the results showed that

48 HULIS accounted for 5.3% of smoke $PM_{2.5}$ (Fan et al., 2016). Unfortunately, only a light coal in the shape of

49 honeycomb briquette was tested that did not reflect the variety of coal types and forms actually being used for

50 residential heating and cooking in China. Another possible primary HULIS source is vehicle exhaust although there is

51 uncertainty in the importance of this source (El Haddad et al., 2009; Salma et al., 2007; Lin et al., 2010b; Kuang et al.,

52 2015). No direct evidence of primary HULIS in vehicle exhaust has been reported. Secondary processes, including

53 formation in the cloud droplets, heterogeneous or aerosol–phase reactions, can be important sources of HULIS (Lin et

54 al., 2010b; Zheng et al., 2013).

55 Previous studies of HULIS source identification were generally based on the relationship between HULIS and the

56 tracers for specific sources (such as K, levoglucosan, Cl⁻, etc.) (Voliotis et al., 2017; Tan et al., 2016; Lin et al, 2010;

57   Park and Son, 2016; Baduel et al., 2010). Those correlation analyses between HULIS and some species may provide

58   some information regarding possible source and formation of HULIS. However, they do not provide quantitative source

59   apportionments. To date, studies that quantitatively identify HULIS sources are limited (Kuang et al., 2015; Srivastava

60   et al., 2018). Kuang et al. (2015) applied positive matrix factorization (PMF) to apportion sources of ambient HULIS in

61   the Pearl River Delta (PRD) in Southern China. Their study showed that secondary formation was the most important

62   source of HULIS throughout the year with an annual average contribution of 69% at an urban site. Biomass burning

63   also contributed significantly to ambient HULIS.

64   Thus, information is scarce on the quantitative apportionment of HULIS sources in the more polluted regions in

65   Northern China, especially in the winter when large quantities of coal are consumed for indoor heating. Moreover, a

66   considerable proportion of coal is burned in residential household stoves in rural, suburban and even some urban areas

67   under poor combustion conditions and without any emission controls. This coal combustion results in high air pollutant

68   emissions and high ambient concentrations. Wang et al. (2016) estimated that more than 30 million tons of coal are

69   burned per year in households in just the Beijing, Tianjin, and Hebei (BTH) region in Northern China. Residential

70   sources in the BTH region contributed to 32% and 50% of primary $PM_{2.5}$ emissions over the whole year and in winter,

71   respectively (Liu et al., 2016).

72   The primary goals of this study are to determine whether residential coal combustion is a significant source of ambient

73   HULIS and quantify its contributions to HULIS in Beijing. Given the large vehicle population in Beijing (up to 5.2

74   million in 2012), this study also provides a chance to examine the vehicular emissions contribution to ambient HULIS.

75   Studies included: (1) Characterization of the HULIS emitted from residential coal stoves, vehicle exhaust, and

76   residential biofuel burning; (2) Estimation of anthropogenic primary emission of HULIS based on these source

77   measurements; (3) Measurement of HULIS concentrations and other major species in the ambient urban Beijing $PM_{2.5}$

78   from June 2012 to April 2013; and (4) Application of the source-oriented Community Multiscale Air Quality (CMAQ)

79   model to quantitatively determine the source contributions to HULIS. The information obtained in this study improves

80   our understanding of the characteristics and sources of primary HULIS and the impact of those sources on HULIS in

81   ambient $PM_{2.5}$.

82   **2 Materials and Methods**

83   **2.1 Ambient sampling**

84   Beijing is surrounded by mountains to the west, north, and northeast, and is adjacent to the northwest portion of the

85   North China Plain. It has a warm and semi-humid continental monsoon climate with four distinctive seasons,

Atmospheric
Chemistry
and Physics
Discussions

86 characterized by strong windy and dusty weather in spring, high temperatures and humidity with extensive rain in

87 summer, cool and pleasant weather in autumn, and cold and dry weather in winter. The annual average wind speed is

88 2.5 m s^{-1} with mostly northerly or northwesterly winds in winter and southerly or southeasterly winds in summer.

89 Twenty-four-hour ambient $PM_{2.5}$ samples were collected non-continuously from 14 June 2012 to 2 April 2013 on the

90 campus of Beihang University (BHU, 39°59'N, 116°21'E) (Figure S1). The sampling period covered four seasons with

91 132 samples being collected for HULIS analysis. The site is surrounded by educational and residential districts without

92 major industrial sources. Major nearby roads are the North Fourth Ring Road about 900 m to the north, North Third

93 Ring Road about 1.2 km to the south, and Xueyuan Road about 350 m to the east. Ambient $PM_{2.5}$ sampling instruments

94 were installed on the roof of a building approximately 25 m above the ground level at Beihang University. A

95 high-volume aerosol sampler (RFPS-1287-063, Thermo, USA) was operated at a flow rate of 1.13 m^3 min^{-1} to collect

96 $PM_{2.5}$ samples on prebaked quartz filters (with area 417.6 cm^2) for the determination of water-soluble organic carbon

97 (WSOC) and humic-like substances (HULIS). $PM_{2.5}$ samples were also collected using a 5-channel Spiral Ambient

98 Speciation Sampler (SASS, Met One Inc., USA) with a flow rate of 6.7 L min^{-1}. Wang et al. (2015) provided the details

99 of the sample collection.

100 Meteorological data including wind speed (WS), temperature, relative humidity (RH) and precipitation were obtained

101 from China Meteorological Data Sharing Service System (http://cdc.cma.gov.cn/home.do).

102 **2.2 Source Sampling**

103 Residential biofuel and coal combustion emissions, and vehicle exhaust, which are representative of typical emission

104 sources around Beijing, were sampled in this study.

105 **2.2.1 Residential biofuel and coal combustion**

106 Three typical types of biofuel, i.e. wheat straw, corn stover, and wood, were burned in an improved stove, which has an

107 enclosed combustion chamber and a bottom grate and a chimney. The sampling procedures are described by Li et al.

108 (2007, 2009) and are briefly summarized here. The water boiling test was used to simulate a common cooking

109 procedure. The burning cycle included heating a specific amount of water from room temperature to its boiling point

110 and then letting it simmer for a few minutes. Both the high power and low power phases were included in the burn

111 cycle to simulate cooking practices of a typical household. The sampling period covered the entire cycle and lasted

112 20-30 minutes.

113 Five coal types were selected for source testing covering a wide range of maturity with volatile matter content varying

114 from 9.6% to 32.4%. Two coal stoves were tested, including a high efficiency, heating stove that employs under-fire

115　　combustion technology and a traditional cooking and heating stove that employs over-fire combustion technology (Li et

116　　al., 2016). Four chunk coals and one briquette coal were burned in the high efficiency stove and three chunk coals were

117　　burned in the traditional stove. Coal/stove combinations are presented in Table 2. To reduce the interference from

118　　igniting the fire, coal was ignited with a propane gas flame from a torch. Emission sampling covered from fire start to

119　　fire extinction and lasted two to three hours.

120　　Source testing of residential biofuel and coal combustion was performed at Beihang University. The test fuels were

121　　air-dried, and the results of their proximate and ultimate analyses are listed in Table S1 in SI. An outline of the sampling

122　　system is shown in Fig. S2. The stove was placed into a chamber. Purified air was induced into the chamber with a fan

123　　to provide dilution air. Emissions were extracted from the chimney with an exhaust hood and were diluted with purified

124　　air, cooled to no more than 5 degrees Celsius at ambient temperature, and then drawn through a sampling duct and

125　　exhausted from the laboratory. Both air flows were adjusted using frequency modulators to change fan speeds. The gas

126　　flow velocity in the sampling duct was measured by a pitot tube to be over 5 m/s. Flow was isokinetically withdrawn

127　　from the sampling duct with a probe and directed into the residence chamber. $PM_{2.5}$ samples were collected from the

128　　end of the residence chamber onto prebaked quartz filters with a diameter of 47mm through $PM_{2.5}$ cyclones at a flow

129　　rate of 16.7 liters/min.

130　　**2.2.2 Vehicle exhaust**

131　　Four light-duty gasoline vehicles certified as meeting the China 4 emissions regulations were tested for their emissions

132　　on a chassis dynamometer. The tests were conducted using the New European Driving Cycle (Marotta, et al., 2015) and

133　　lasted 1180 s, including four repeated urban driving cycles and one extra-urban driving cycle. The emissions testing and

134　　sampling system are described in detail by Li et al. (2016) and are briefly summarized here. The vehicle exhaust was

135　　directed into a critical flow Venturi constant volume sampler in a full flow dilution tunnel. The $PM_{2.5}$ samples were

136　　collected on prebaked quartz filters with a diameter of 47mm through $PM_{2.5}$ cyclones at a flow rate of 80 L/min.

137　　Three heavy-duty diesel trucks were selected to perform on-road emission test. The tests were conducted on both

138　　highway and city roads. The emission testing and sampling system are described in detail elsewhere (He et al., 2015)

139　　and are briefly summarized here. A Micro Proportional Sampling System (SEMTECH-MPS; Sensors Inc., MI, USA)

140　　was used to draw a constant ratio of sample flow from exhaust and dilute the sample flow. $PM_{2.5}$ samples were collected

141　　onto prebaked quartz filters with a diameter of 47mm through $PM_{2.5}$ cyclones at a flow rate of 10 liters/min.

142　　Tunnel measurements was also conducted to collect vehicle exhaust at the Badaling Tunnel in Beijing. The length of the

143　　tunnel is 1085 m. The ventilation in the tunnel was achieved by the flow of the traffic induced into the tunnel during the

144　　sampling period. $PM_{2.5}$ samplers with prebaked 47mm quartz filters were operated at a flow rate of 16.7 L/min at the

145   inlet and the outlet of the tunnel simultaneously. The sampling period was 2 hours and the samples represent the mixed

146   exhaust of gasoline-fueled vehicles and diesel-fueled vehicles.

147   All source samples collected on the quartz filters were analyzed for HULIS, WSOC and OC/EC according the methods

148   described in Section 2.3.

2.3 Chemical Characterization

150   HULIS isolation was based on the extraction method developed by Varga et al. (2001) and used in many other studies

151   (Nguyen et al., 2014; Lin et al., 2010b; Fan et al., 2012; Song et al., 2012; Lin et al., 2011; Salma et al., 2013; Feczko et

152   al., 2007; Krivácsy et al., 2008). The separation procedure is provided in SI Text S1. WSOC and $HULIS_C$ were

153   determined using a total organic carbon (TOC) analyzer (Shimadzu TOC-Vcph, Japan) based on a

154   combustion-oxidation, non-dispersive infrared absorption method. The TOC was determination by subtracting inorganic

155   carbonate (IC) from total carbon (TC): TOC = TC - IC. The reported data were the average results of three replicate

156   measurements. Mass concentrations of HULIS were obtained from $HULIS_C$ by multiplying a scaling factor of 1.9 as

157   suggested by Lin et al. (2012a), Kiss et al. (2002), and Zheng et al. (2013).

158   A 0.5 cm^2 punch from each quartz filter was analyzed for OC and EC using a DRI Model 2001 Thermal/Optical Carbon

159   Analyzer (Atmoslytic Inc., Calabasas, USA) following the IMPROVE-A thermal optical reflectance (TOR) protocol

160   (Chow et al., 2007).

161   The $PM_{2.5}$ samples from SASS were also analyzed for mass, water-soluble inorganic ions analysis as described by

162   Wang et al. (2015).

2.4 CMAQ modelling of primary HULISc

164   A source-oriented version of the Community Multiscale Air Quality (CMAQ) model (version 5.0.1) was used in this

165   study to track primary $PM_{2.5}$ ($PPM_{2.5}$) from different emission sectors and determine the resulting concentrations of

166   primary HULIS. The model was used in a previous study to determine source contributions to $PPM_{2.5}$ mass, EC and

167   primary OC (POC) in China. Details of the source apportionment technique can be found in Hu et al (2015). In

168   summary, source contributions to $PPM_{2.5}$ mass were directly determined using non-reactive source-specific tracers to

169   track the emissions of $PPM_{2.5}$ from different sources. These non-reactive tracers were treated identically to the other

170   PPM components when simulating their emission, transport, and removal. A constant scaling factor (typically 10^{-4} or

171   10^{-5}) was used to scale the actual emission rate of these tracers to ensure that their concentrations are sufficiently low

172   that they do not alter the removal rates of other PM components. The concentrations and source contributions to EC and

173   POC were determined during post-processing by using source-specific emission factors as well as the model predicted

174   source contributions to $PPM_{2.5}$ mass concentrations. This technique can be used to determine source contributions to

175   primary HULIS. For example, contributions of the ith emission source to primary HULISc concentration ($HULISc_{,i}$) can

176   be calculated using equation (1):

177    $HULISc_{,i}=PPM_{2.5,i}*f_{OC,i}*f_{HULIS,i}$ (1)

178   where $f_{HULIS,i}$ is the mass fraction of HULIS per unit emission of POC from the ith source (see Section 3.3 below for

179   estimation of HULIS primary emission) and $f_{OC,i}$ is the mass fraction of POC per unit emission of $PPM_{2.5,i}$ from the ith

180   source, and $PPM_{2.5,i}$ is the calculated source contributions to $PPM_{2.5}$ from the ith source based on the non-reactive tracer.

181   The total concentration of primary HULIS can be determined by adding the primary HULIS contributions from the

182   different sources.

183   In this study, the model uses a 36 km × 36 km horizontal resolution to cover a rectangular domain that includes all of

184   China and neighboring countries. Source contributions to HULIS were calculated for the periods when observations of

185   HULIS are available. Emissions from anthropogenic source sectors (residential sources, power plants, industries, and

186   transportation) are based on Multi-resolution Emission Inventory of China (MEIC) 2012 (www.meicmodel.org). Open

187   biomass burning was estimated using the FINN dataset from the National Center for Atmospheric Research (NCAR)

188   (Wiedinmyer et al., 2011). Natural emissions from soil erosion and sea spray were modeled within the CMAQ model

189   (Appel et al., 2013; Kelly et al., 2010). Biogenic emissions were estimated using the Model for Emissions of Gases and

190   Aerosol from Nature (MEGAN) version 2.10. Meteorological fields were calculated using the Weather Research and

191   Forecasting (WRF) model. Details of the model setup, input data preparation, as well as model evaluation for $PPM_{2.5}$

192   mass are documented by Hu et al (2015). In this study, a comparison of predicted daily $PPM_{2.5}$ concentrations with

193   observations was performed and only those predictions with fractional errors (FE) less than 0.6 were included in the

194   calculation of primary HULIS. The values of f_{OC} for different source sectors used in the calculation are included in SI

195   Table S3. These values were used in Ying et al. (2018), and the predicted daily-average POC and EC concentrations

196   generally agree with predictions for both daily and annual average concentrations.

197   **3 Results and discussion**

198   **3.1 General of ambient aerosol characteristics**

199   The concentrations of $PM_{2.5}$, carbonaceous species (OC, EC, WSOC and HULIS), and inorganic ions such as SO_4^{2-},

200   NO_3^-, NH_4^+, and K^+ are summarized in Table 1. The 24-hour average $PM_{2.5}$ concentration for the sample set was 106 ±

201   89 $\mu g/m^3$, about three times the national annual air quality standard (35 $\mu g/m^3$). The highest concentration (~600 $\mu g/m^3$)

202   appeared on 12-13 January 2013 as reported in other studies (Quan et al., 2014; Tian et al., 2014; Zheng et al., 2015).

Atmospheric
Chemistry
and Physics
Discussions
Open Access
EGU

203 The severe pollution events were always accompanied by high relative humidity and low wind speeds (Fig. 1). During

204 the entire sampling period, severely polluted days (PM$_{2.5}$ concentrations $\geq$ 150 µg/m^3) constituted about 22%, while fair

205 days (PM$_{2.5}$ concentrations $\leq$ 75 µg/m^3) approached 50%. The average PM$_{2.5}$ concentrations in summer, autumn, winter,

206 and spring were 98 ± 60 µg/m^3, 58 ± 48 µg/m^3, 150 ± 121 µg/m^3, and 120 ± 76 µg/m^3, respectively.

207 The average HULIS concentration for the study period was 7.5 ± 7.8 µg/m^3. This value is lower than the average

208 value of 11.8 µg/m^3 measured at a rural site in the PRD region that was heavily influenced by biomass burning (Lin et

209 al., 2010b). However, it is higher measurements in the urban areas (about 5 µg/m^3) in the PRD (Lin et al., 2010a; Kuang

210 et al., 2015), urban Shanghai (about 4 µg/m^3) (Zhao et al., 2015), and urban Lanzhou (about 4.7 µg/m^3) (Tan et al.,

211 2016). HULIS exhibited obvious seasonal variations as shown in Figure 1 and Table 1. The seasonal average

212 concentrations were 5.5 ± 4.4 µg/m^3, 5.6 ± 4.7 µg/m^3, 12.3 ± 11.7 µg/m^3, and 6.5 ± 5.5 µg/m^3 in summer, autumn,

213 winter, and spring, respectively. The winter mean was about twice the value in any other season, and the highest

214 concentration (54.96 µg/m^3) of HULIS was observed on the same day that the highest concentration of PM$_{2.5}$ was

215 observed. The mean HULIS concentrations were very similar between summer and autumn in contrast with PM$_{2.5}$ that

216 has much higher concentrations in the summer (Table 1). These seasonal variations were similar with those observed in

217 Aveiro and K-puszta (Feckzo et al., 2007), but those annual average concentrations (about 2.4 µg/m^3 and 3.2 µg/m^3,

218 respectively) were much lower than in Beijing. The concentrations of HULIS in previously reported studies are

219 summarized in Supporting Table S1.

220 HULIS and PM$_{2.5}$ had a significant positive correlation with the annual r^2=0.90 (r^2 = 0.77, 0.96, 0.96 and 0.94 in

221 summer, autumn, winter, and spring, respectively) (Figure S4a). The seasonal average of HULIS/PM$_{2.5}$ was 5.9%, 9.4%,

222 7.9%, and 4.8% in summer, autumn, winter, and spring, respectively. The annual average of HULIS/PM$_{2.5}$ was 7.2% ±

223 3.3%, lower than the ~10% in the PRD region (Lin et al., 2010a).

224 Strong correlations of HULIS$_C$ with OC were observed with the annual r^2=0.87 (r^2 = 0.94, 0.82, 0.89 and 0.84 in

225 summer, autumn, winter, and spring, respectively) (Fig S4c). The percentage of HULIS$_C$ in OC for summer, autumn,

226 winter, and spring, respectively, were 29.2 ± 6.2%, 26.2 ± 9.6%, 21.0 ± 7.1%, and 22.0 ± 6.9% with an annual average

227 of 24.5% ± 8.3%.

228 Strong correlations of HULIS$_C$ with WSOC were also observed with the annual r^2=0.98 (r^2 = 0.99, 0.96, 0.99 and 0.98

229 in summer, autumn, winter, and spring, respectively) (Figure S4b). The percentage of HULIS$_C$ in WSOC for summer,

230 autumn, winter, and spring, respectively, were 66.7 ± 5.4%, 54.1% ± 11.2%, 62.3% ± 5.7% and 56.6% ± 6.3% with an

231 annual average of 59.5% ± 9.2%, suggesting that HULIS$_C$ was the major constituent of WSOC. This value is

232 comparable to the results (about 60%) at urban sites in the PRD region (Lin et al., 2010b; Fan et al., 2012), Shanghai

Atmospheric
Chemistry
and Physics
Discussions

233   (Zhao et al., 2015), Korea (Park et al., 2012), Budapest (Salma et al., 2007; 2008; 2010), and high-alpine area of the

234   Jungfraujoch, Switzerland (Krivácsy et al., 2001). However, it is higher than the rural areas in K-puszta, Hungary

235   (Salma et al., 2010) and the northeastern US (Pavlovic and Hopke, 2012). The ratios of $HULIS_C$/WSOC reported by

236   previous studies are listed in Supporting Table S1.

3.2 HULIS emission characteristics from various sources

238   The measured $HULIS_C$/OC (i.e. $f_{HULIS,i}$), $HULIS_C$/WSOC from the source samples are presented in Table 2. Biomass

239   combustion produces a significant fraction of HULIC in OC (0.41-0.50) whether burning wood or crop straw. Those

240   values are high compared to previous studies. The $HULIS_C$/OC values obtained by Lin et al., (2010a, 2010b) were 0.14

241   to 0.34 from rice straw and sugarcane burning in the PRD region in south China. Park and Yu (2016) found the ratios

242   from burning rice straw, pine needles, and sesame stems in Korea were in the range of 0.15 to 0.29. Schmidl et al.

243   (2018a, 2018b) reported the ratios of 0.01-0.12 for wood burning and 0.33-0.35 for leaves burning in the mid-European

244   Alpine region. Goncalves et al. (2010) obtained ratios of 0.04 to 0.11 from wood burning in Portugal. HULIS is an

245   important component of WSOM. High $HULIS_C$/WSOC ratios (0.62 to 0.65) were observed for three types of biomass

246   burning in this study. These results are comparable with two previous studies. Fan et al. (2017) reported the ratios from

247   burning rice straw, corn straw, and pine branch were in the range of 0.57 to 0.66. Park and Yu (2016) obtained ratios in

248   the range of 0.36 to 0.63 from burning three types of biomass. However, Lin et al. (2010a) reported relatively low

249   values ranging from 0.30 to 0.33 from rice straw and sugarcane burning.

250   Residential coal combustion produces 5 to 24% of the OC as HULIS for all the coal/stove combinations in this study.

251   Only one prior study measured HULIS emitted from residential honeycomb coal briquette combustion (Fan et al., 2016).

252   However, the HULIS to OC ratio was not reported in that study. HULIS/WSOM ratio (0.46) in that study are

253   comparable with our $HULIS_C$/WSOC data (0.41-0.62).

254   Light-duty gasoline and heavy-duty diesel vehicles also produced primary HULIS on the order of 5 to 16% of the

255   emitted OC. The HULIS content detected in the vehicle exhaust samples was generally less than the detection limit for

256   these measurements. Thus, these reported ratios of $HULIS_C$ to OC for vehicle emissions have high uncertainties. Ratios

257   of $HULIS_C$ to OC for vehicle emissions obtained in this study are much higher than prior tunnel measurements (2-5%)

258   (El Haddad et al. 2009). However, they are comparable with those from residential coal combustion. Due to more

259   complete combustion or more advance emission controls in vehicles than residential solid fuel combustion, OC

260   emission factors for vehicles are normally around two orders of magnitude less than that for residential coal combustion

261   (MEP of China, 2014), so HULIS emission from vehicles can be neglected as described in Section 3.3.

Atmospheric
Chemistry
and Physics
Discussions

262 **3.3 Estimation of HULIS primary emission**

263 The average values of $f_{HULIS,i}$ for residential biofuel and coal combustion, and vehicle exhaust obtained from our

264 measurement were used for to assess the extent of primary emissions. Due to lack of $f_{HULIS,i}$ for the other sectors, such

265 as power plants and industries, considering combustion/production technology and emission control technology, we

266 assumed values for these two sectors as 0.01 and 0.05, respectively.

267 Based on OC emissions for different sources in the MEIC inventory and the $f_{HULIS,i}$ for the various sources described

268 above, the annual anthropogenic primary emission of HULIS in Beijing is estimated to be approximately 6.3 Gg with

269 over 60 percent of this primary HULIS being emitted during the heating season. Residential biomass and coal burning

270 contribute about 70% and 25% of the annual primary HULIS emissions, respectively. Vehicle exhaust contributions to

271 annual primary HULIS emission are negligible (less than 2%). While industry sector and power plants contribute about

272 3% and close to zero, respectively. In winter, residential biomass and coal burning contribute close to 98 percent of

273 primary HULIS (Supporting Table S3).

274 Terrestrial and marine emissions were not included in these estimations of primary HULIS emissions since they were

275 considered to be negligible for inland cities, such as Beijing (Graber and Rudich, 2006; Zheng et al., 2013).

276 **3.4 Possible primary sources and secondary formation of HULIS**

277 Ambient HULIS sources include primary sources and atmospheric secondary processes that convert gaseous precursors

278 to HULIS. The correlation between HULIS and other measured constituents provide information regarding possible

279 sources and formation mechanisms of HULIS.

280

Atmospheric
Chemistry
and Physics
Discussions

3.4.1 HULIS from primary sources

281

282 Correlations between HULIS and primary species in $PM_{2.5}$ are shown in Figure 2. POC and secondary organic carbon

283 (SOC) were estimated using the EC tracer method (Lim and Turpin, 2002; Turpin and Huntzicker, 1995). The details of

284 the method and evaluation are provided in Text S2. Figures 2a and 2b show that there are strong correlations between

285 HULIS and POC, and HULIS and EC throughout the year indicating that HULIS has sources and/or transport processes

286 similar to those of POC and EC. Both POC and EC are co-emitted by the incomplete combustion of carbon-containing

287 fuels. According to the 2010 MEIC data for Beijing 2010, biomass and residential coal burning contribute more than 80

288 percent of the POC emissions, the industrial sector contributes over 10 percent, and vehicular exhaust contributions are

289 negligible. For EC emission, residential coal burning contributes more than 50 percent, biomass burning, industry, and

290 vehicles contributes the rest.

291 K^+ generally originate from biomass burning with lesser contributions from coal burning and dust. However, biomass

292 burning is regarded as the most important source for K^+ and it is often used as an indicator of biomass burning (Kuang

293 et al., 2016; Zhang et al., 2013; Park et al., 2015; Pio et al., 2008; Wang et al., 2011; 2012; Cheng et al., 2013). In North

294 China, biomass burning occurred in all seasons including residential cooking, heating, and open biomass burning

295 (Cheng et al., 2013; Zheng et al., 2015). High K^+ concentrations in this study were observed with mean values of 2.2 ±

296 2.9 $\mu g/m^3$, 1.3 ± 1.0 $\mu g/m^3$, 3.2 ± 3.6 $\mu g/m^3$ and 2.2 ± 1.3 $\mu g/m^3$ in summer, autumn, winter, and spring, respectively,

297 and an annual average of 2.2 ± 2.6 $\mu g/m^3$. As shown in Figure 3c, HULIS and K^+ exhibited a strong correlation with

298 r^2=0.76, 0.73, and 0.61 in summer, autumn, and spring, respectively, suggesting the contribution of biomass burning to

299 HULIS. During the winter sampling period, a low correlation was initially obtained (r^2 = 0.21). However, two extreme

300 values of K^+ were observed on New Year's Eve (February 9, 2013, 14.6 $\mu g/m^3$) and Lantern Festival (February 24, 2013,

301 17.6 $\mu g/m^3$). Prior studies had suggested that fireworks during the Spring Festival and Lantern Festival produce very

302 high K^+ concentrations (Shen et al., 2009; Jing et al., 2014; Jiang et al., 2015). Excluding these two days (red points in

303 Figure 2c), the correlation between HULIS and K^+ increased to r^2=0.73, indicating the contribution of biomass burning

304 to HULIS in winter. The strong correlation coefficient between HULIS and K^+ across all the seasons also confirmed that

305 biomass burning was a significant primary HULIS emission source as presented in the Section 3.3.

306 Cl^- is usually believed to be associated with coal combustion and biomass burning (Yu et al., 2013; Gao et al., 2015;

307 Yao et al., 2002; Li et al., 2007; Li et al., 2009). A significant contribution from sea-salt particles for Cl^- in $PM_{2.5}$ can be

308 excluded since the average mole ratios of Cl^- to Na^+ across four seasons in this study is 5.0, much higher than the ratio

309 in seawater of 1.17. Moreover, the sampling site in Beijing is about 200 Km from the sea. The correlation of HULIS

310 and Cl^- is shown in Fig. 2d. In winter and spring, HULIS is moderately correlated with Cl^- with r^2=0.56 and r^2=0.64,

Atmospheric
Chemistry
and Physics
Discussions

311   respectively. While weaker correlations were observed in summer and autumn with r^2=0.40 and r^2=0.43, respectively.

312   This result reflects the different amounts of coal burned in specific seasons. In winter and spring in northern China, coal

313   combustion for heating was quite prevalent and more coal was burned compared to the other two seasons, resulting in

314   the substantial emissions of gaseous and particulate pollutants, including HULIS and Cl$^-$. The source study in Section

315   3.2 found that HULIS contributed to about 12% of OC emitted from residential coal combustion. The correlation

316   coefficient between HULIS and Cl$^-$ in winter and spring provides additional support for coal burning being an important

317   primary HULIS emission source as discussed in Section 3.3. The strong correlation between HULIS and Cl$^-$ in winter

318   (R^2=0.89) and weak correlation in summer (R^2=0.17) were also revealed in Lanzhou, another city in northern China

319   (Tan et al., 2016). Significant correlation between HULIS and Cl$^-$ in wintertime urban aerosols from central and

320   southern Europe were also found (Voliotis et al., 2017). The authors suggest the high concentration of HULIS during

321   winter was probably related with residential coal burning (Tan et al., 2016; Voliotis et al., 2017).

322   Ca^{2+} would be more likely originated from the re-suspended road dust and long-range transported dust (Gao et al.,

323   2014). The poor correlation between HULIS and Ca^{2+} (as shown in Figure 2e) indicated dust was not likely to be an

324   important source of HULIS.

325   **3.4.2 HULIS associated with atmospheric secondary processes**

326   The correlations between HULIS and related secondary species are shown in Figure 3. As shown in Figure 3a and 3b,

327   HULIS correlated well with SO_4^{2-} and SOC (R^2=0.68 for HULIS and SO_4^{2-} and R^2=0.61 for HULIS and SOC),

328   suggesting that HULIS and secondary species may have similar formation pathways. Moderate to strong correlations of

329   HULIS and SO_4^{2-}, and HULIS and SOC were observed in autumn and winter, but with significant differences in the

330   concentrations. The lower temperature and solar intensity in winter were not conducive to the photochemical formation

331   of secondary aerosols, but high relative humidity and stable synoptic meteorological conditions accompanied with

332   heterogeneous reactions probably played a role in the formation of secondary aerosols (Zheng et al., 2015). In summer,

333   HULIS was strongly correlated with SOC (R^2=0.85), while weakly correlated with SO_4^{2-} (R^2=0.41), indicating the

334   distinct formation processes of HULIS and SO_4^{2-}. High temperature and solar radiation accelerated the photochemical

335   reactions between oxidants and organic precursors (Lin et al., 2010). However, a moderate correlation of HULIS &

336   SO_4^{2-} (R^2=0.36) but unfavorable correlation between HULIS and SOC (R^2=0.10) were acquired in spring, suggesting

337   the different formation pathways of HULIS and SOA.

338   **3.5 HULIS source apportionment based on CMAQ modelling**

339   CMAQ predicted concentrations of $PPM_{2.5}$ from different sources were used to calculate HULISc from these sources

340   using equation (1). The total concentration of primary HULIS can be determined by adding up primary HULIS from

341   different sources. Figure 4 shows the predicted primary HULISc and observed HULISc concentrations with the

342   prediction uncertainty. Only days with acceptable PPM$_{2.5}$ performance were shown in the Figure 4. Primary HULISc in

343   January and March 2013 accounts for almost all observed HULISc in these two months. In summer and autumn 2012,

344   predicted primary HULISc concentrations are approximately 1-2 μg m^{-3}. There were days when the observed HULISc

345   concentrations were much higher than predicted primary HULISc concentrations indicating potential contributions of

346   secondary HULISc.

347   Table 3 shows the seasonal contributions for each source as well as average source contributions for the whole sampling

348   period to ambient HULIS in Beijing based on the observed total HULISc and CMAQ predicted primary HULISc on the

349   days with acceptable PPM$_{2.5}$ performance. Contributions of HULISc from secondary processes were determined by

350   subtracting predicted primary HULISc from observed HULISc. For those days when the predicted primary HULISc

351   concentrations are greater than the observed HULISc, the predicted primary HULISc concentrations were set to equal

352   the observed HULISc and the secondary HULISc were set to zero. Based on the HULIS emissions from residential

353   biofuel and coal burning described in Section 3.3, the contributions of biofuel and coal burning in the residential sector

354   to ambient HULIS were estimated separately.

355   Overall, residential biofuel burning was the most important source of ambient HULIS, contributing more than half of

356   the ambient HULIS concentrations, much higher than those results from the PRD in Southern China (less than 20%)

357   (Kuang et al. 2015). This difference is likely with the result of greater biofuel burning during the heating seasons in the

358   Beijing area. Residential coal burning contributes 12.3±2.8% to ambient HULIS and is also a significant source of

359   ambient HULIS. A large contribution from residential sector to ambient HULIS is consistent with the estimation of

360   HULIS primary emission and the correlations between HULIS and primary species previously presented. Vehicle

361   emissions and other primary sources, such as industries, contribute negligible amounts to the ambient HULIS.

362   Contributions from the residential sector display strong seasonal variations. In winter and spring, residential biofuel and

363   coal burning accounted for over 80% of the total HULISc while their contributions were reduced to approximately 40%

364   in summer and autumn. The seasonal variations were a reflection of seasonal pattern of those activities in this region.

365   Secondary formation is estimated to have contributed an average of 25.8±9.3% to the HULIS concentrations and was

366   another major source to ambient HULIS as indicated by the correlations between HULIS and secondary species (i.e.

367   SNA, SOC). However, our result is much lower than those results from PRD in Southern China (55 to 69%) (Kuang et

368   al. 2015). The difference is driven by the differences in sources and climatological patterns between these two sites.

369   There is much greater combustion for space heating in the colder north and atmospheric reaction rates will be higher in

370   the warmer south. Contributions from secondary processes also show obvious seasonal variations trend. In winter and

371   spring, secondary processes accounted for less than 20% of the total HULISc with large uncertainties while their

372   contributions were increased to 40±18% and 53±17% in summer and autumn. Higher secondary contributions were also

373   found during warm seasons in the PRD region (Kuang et al. 2015). In addition to the proposed heterogeneous

374   secondary formation pathways for HULISc, oxidation reactions initiated by chlorine (Cl) radicals can form SOA (Wang

375   and Ruiz, 2017; Riva et al., 2015). Thus, Cl release by coal combustion may have the potential to contribute to HULISc,

376   especially during winter when OH radical concentrations are much lower (monthly average 5.5×10^{-3} ppt for winter vs.

377   1.25×10^{-1} ppt for summer based on CMAQ calculations for Beijing). However, the concentrations of secondary

378   HULISc for winter estimated in this study are uncertain (1.8 ± 2.2 µg m^{-3}) compared to the summer time average

379   concentration (1.0 ± 0.4 µg m^{-3}). Therefore, the role of Cl initiated reactions producing HULISc cannot be definitively

380   determined.

381   Figure 5 shows scatter plot of predicted primary HULISc vs observed HULISc concentrations. Moderate to strong

382   correlations between predicted primary HULISc were observed in winter and spring, while relatively weaker correlations

383   were found in autumn. Moreover, low correlations were observed in summer. The variation of correlation coefficient

384   between predicted primary HULISc and observed HULISc in different seasons also provides additional support for the

385   relative importance of primary and secondary HULIS as shown in Table 3.

386   **Supporting Information**

387   The supporting information file for this paper provides the details of HULIS analytical procedures, and prior literature

388   regarding HULIS in the ambient aerosol. It also provides some additional figures and descriptions that help to support

389   the analyses and discussion presented in the paper.

390   **Acknowledgment**

395   **References**

396   Appel, K.W., Pouliot, G.A., Simon, H., Sarwar, G, Pye, H.O.T., Napelenok, S.L., Akhtar, F., and Roselle, S.J.:

397   Evaluation of dust and trace metal estimates from the Community Multiscale Air Quality (CMAQ) model version

398   5.0, Geosci. Model Dev. Discuss., 6, 1859-1899, 2013.

399   Baduel, C., Voisin, D., and Jaffrezo, J. L.: Seasonal variations of concentrations and optical properties of water soluble

400   HULIS collected in urban environments, Atmos. Chem. Phys., 10, 4085-4095, 2010.

401   Beine, H., Anastasio, C., Esposito, G., Patten, K., Wilkening, E., Domine, F., Voisin, D., Barret, M., Houdier, S., and

402   Hall, S.: Soluble, light absorbing species in snow at Barrow, Alaska, J. Geophys. Res., 116, D00R05,

403   doi:10.1029/2011JD016181, 2011.

404   Cheng, Y., Engling, G., He, K.B., Duan, F.K., Ma, Y.L., Du, Z.Y., Liu, J.M., Zheng, M., and Weber, R.J.: Biomass

405   burning contribution to Beijing aerosol, Atmos. Chem. Phys., 13, 7765–7781, 2013.

406   Chow, J.C., Watson, J.G, Chen, L.W.A., Chang, M.C.O., Robinson, N.F., Trimble D., and Kohl, S.: The IMPROVE-A

407   Temperature Protocol for Thermal/Optical Carbon Analysis: Maintaining Consistency with a Long-Term Database,

408   J. Air Waste Manage., 57, 1014–1023, 2007.

409   Dinar, E., Taraniuk, I., Graber, E.R., Katsman, S., Moise, T., Anttila, T., Mentel, T.F., and Rudich, Y.: Cloud

410   condensation nuclei properties of model and atmospheric HULIS, Atmos. Chem. Phys., 6, 2465-2481, 2006.

411   El Haddad, I., Marchand, N., Dron, J., Temime-Roussel, B., Quivet, E., Wortham, H., Jaffrezo, J.-L., Baduel, C., Voisin,

412   D., Besombes, J., and Gille, G: Comprehensive primary particulate organic characterization of vehicular exhaust

413   emissions in France, Atmos. Environ., 43, 6190-6198, 2009.

414   Fan, X., Wei, S., Zhu, M., Song, J., and Peng, P.: Comprehensive characterization of humic-like substances in smoke

415     $PM_{2.5}$ emitted from the combustion of biomass materials and fossil fuels, Atmos. Chem. Phys., 16, 13321–13340,

416   2016.

417   Fan, X.J., Song, J.Z., and Peng, P.A.: Comparison of isolation and quantification methods to measure humic-like

418   substances (HULIS) in atmospheric particles, Atmos. Environ., 60, 366-374, 2012.

419   Feczko, T., Puxbaum, H., Kasper-Giebl, A., Handler, M., Limbeck, A., Gelencsér, A., Pio, C., Preunkert, S., and

420   Legrand, M.: Determination of water and alkaline extractable atmospheric humic-like substances with the TU

421   Vienna HULIS analyzer in samples from six background sites in Europe, J. Geophys. Res., 112. D23S10, 2007.

422   France, J.L., King, M.D., Frey, M.M., Erbland, J., Picard, G, Preunkert, S., MacArthur, A., and Savarino, J.: Snow

423   optical properties at Dome C (Concordia), Antarctica, implications for snow emissions and snow chemistry of

424   reactive nitrogen, Atmos. Chem. Phys., 11, 9787–9801, 2011.

425   France, J.L., Reay, H.J., King, M.D., Voisin, D., Jacobi, H.W., Domine, F., Beine, H., Anastasio, C., MacArthur, A., and

426   Lee-Taylor, J.: Hydroxyl radical and NOx production rates, black carbon concentrations and light-absorbing

427 impurities in snow from field measurements of light penetration and nadir reflectivity of onshore and offshore

428 coastal Alaskan snow, J. Geophys. Res., 117, D00R12, 2012.

429 Gao, J., Tian, H., Cheng, K., Lu, L., Zheng, M., Wang, S., Hao, J., Wang, K., Hua, S., Zhu, C., and Wang, Y.: The

430 variation of chemical characteristics of $PM_{2.5}$ and PM_{10} and formation causes during two haze pollution events in

431 urban Beijing, China, Atmos. Environ., 107, 1-8, 2015.

432 Gao, J.J., Tian, H.Z., Chen, K., Wang, Y.X., Wu., Y. and Zhu, C.Y.: Seasonal and spatial variation of trace Elements in

433 Multi-Size Airborne particulate Matters of Beijing, China: Mass Concentration, Enrichment Characteristics,

434 Source Apportionment, Chemical Speciation and Bioavailability, Atmos. Environ., 99: 257–265, 2014.

435 Ghio, A. J., Stonehuerner, J., Pritchard, R. J., Piantadosi, C. A., Quigley, D. R., Dreher, K. L., and Costa, D. L.:

436 Humic-like substances in air pollution particulates correlate with concentrations of transition metals and oxidant

437 generation, Inhalation Toxicol., 8, 479–494, 1996.

438 Goncalves, C., Alves, C., Evtyugina, M., Mirante, F., Pio, C., Caseiro, A., Schmidl, C., Bauer, H., and Carvalho F.:

439 Characterisation of PM_{10} emissions from woodstove combustion of common woods grown in Portugal, Atmos.

440 Environ., 44(35): 4474-4480, 2010.

441 Graber, E.R. and Rudich, Y.: Atmospheric HULIS: How humic-like are they? A comprehensive and critical review,

442 Atmos. Chem. Phys., 6, 729-753, 2006.

443 Gysel, M., Weingartner, E., Nyeki, S., Paulsen, D., Baltensperger, U., Galambos, I., and Kiss, G: Hygroscopic

444 properties of water-soluble matter and humic-like organics in atmospheric fine aerosol, Atmos. Chem. Phys., 4,

445 35-50, 2004.

446 He L. Q., Hu J. N., and Zu L.: Emission characteristics of exhaust $PM_{2.5}$ and its carbonaceous components from China

447 to China heavy-duty diesel vehicles, Acta Scientiae Circumstantiae, 35(3), 656-662, 2015 (in Chinese).

448 Hoffer, A., Gelencs´er, A., Guyon, P., Kiss, G, Schmid, O., Frank, G P., Artaxo, P., and Andreae, M. O.: Optical

449 properties of humic-like substances (HULIS) in biomass-burning aerosols, Atmos. Chem. Phys., 6, 3563–3570,

450 2006.

451 Hu, J., Wu, L., Zheng, B., Zhang, Q., He, K., Zhang, Q., Li, X., Yang, F., Ying Q., and Zhang, H.: Source contributions

452 and regional transport of primary particulate matter in China, Environ. Pollut., 207, 31-42, 2015.

453 Jiang, Q., Sun, Y.L., Wang, Z., and Yin, Y.: Aerosol composition and sources during the Chinese Spring Festival:

454 fireworks, secondary aerosol, and holiday effects, Atmos. Chem. Phys., 15, 6023-6034, 2015.

455 Jing, H., Li, Y.F., Zhao, J.T., Li, B., Sun, J.L., Chen, R., Gao, Y.X., and Chen, C.Y.: Wide-range particle characterization

456 and elemental concentration in Beijing aerosol during the 2013 Spring Festival, Environ. Pollut., 192, 204-211,

Atmospheric
Chemistry
and Physics
Discussions

Open Access

EGU

457   2014.

458   Kelly, J.T., Bhave, P.V., Nolte, C.G, Shankar, U., and Foley, K.M.: Simulating emission and chemical evolution of

459   coarse sea-salt particles in the Community Multiscale Air Quality (CMAQ) model, Geosci. Model Dev. 3, 257-273,

460   2010.

461   Kiss, G., Varga, B., Galambos, I., and Ganszky, I.: Characterization of water-soluble organic matter isolated from

462   atmospheric fine aerosol, J. Geophys. Res., 107, 8339, 2002.

463   Krivácsy, Z., Gelencsér, A., Kiss, G., Mészáros, E., Molnár, Á., Hoffer, A., Mészáros, T., Sárvári, Z., Temesi, D.,

464   Varga, B., Baltensperger, U., Nyeki, S., and Weingartner, E.: Study on the chemical character of water soluble

465   organic compounds in fine atmospheric aerosol at the Jungfraujoch, J. Atmos. Chem., 39, 235-259, 2001.

466   Krivácsy, Z., Kiss, G., Ceburnis, D., Jennings, G., Maenhaut, W., Salma, I., and Shooter, D.: Study of water-soluble

467   atmospheric humic matter in urban and marine environments, Atmos. Res., 87, 1-12, 2008.

468   Kuang, B. Y., Lin, P., Huang, X. H. H., and Yu, J. Z.: Sources of humic-like substances in the Pearl River Delta, China:

469   positive matrix factorization analysis of PM$_{2.5}$ major components and source markers, Atmos. Chem. Phys., 15,

470   1995-2008, 2015.

471   Li, Q., Jiang, J., Qi, J., Deng, J., Yang, D., Wu, J., Duan, L., and Hao, J.: Improving the energy efficiency of stoves to

472   reduce pollutant emissions from household solid fuel combustion in China, Environ. Sci. Technol. Lett., 3,

473   369-374, 2016.

474   Li, X., Wang, S., Duan, L., Hao, J., and Nie, J.: Carbonaceous aerosol emissions from household biofuel combustion in

475   China, Environ. Sci. Technol., 43: 6076-6081, 2009.

476   Li, X., Wang, S., Duan, L., Hao, J., Li, C., Chen, Y., and Yang, L.: Particulate and Trace Gas Emissions from Open

477   Burning of Wheat Straw and Corn Stover in China, Environ. Sci. Technol., 41, 6052-6058, 2007.

478   Li, Y., Li, Z., and Hu, J.: Emission profile of exhaust PM$_{2.5}$ from light-duty gasoline vehicles, Research of

479   Environmental Sciences, 29(4): 503-508, 2016 (in Chinese).

480   Lim, H. J. and Turpin, B. J.: Origins of primary and secondary organic aerosol in Atlanta: Results' of time-resolved

481   measurements during the Atlanta supersite experiment, Environ. Sci. Technol., 36, 4489–4496, 2002.

482   Lin, P. and Yu, J.Z.: Generation of Reactive Oxygen Species Mediated by Humic-like Substances in Atmospheric

483   Aerosols, Environ. Sci. Technol., 45, 10362-10368, 2011.

484   Lin, P., Engling, G, and Yu, J.Z.: Humic-like substances in fresh emissions of rice straw burning and in ambient

485   aerosols in the Pearl River Delta Region, China. Atmos. Chem. Phys., 10, 6487-6500, 2010.

486   Lin, P., Huang, X.F., He, L.Y., and Yu, J.Z.: Abundance and size distribution of HULIS in ambient aerosols at a rural

487   site in South China, J. Aerosol Sci., 41, 74–87, 2010.

488 Lin, P., Rincon, A.G, Kalberer, M., and Yu, J.Z.: Elemental Composition of HULIS in the Pearl River Delta Region,

489   China: Results Inferred from Positive and Negative Electrospray High Resolution Mass Spectrometric Data,

490   Environ. Sci. Technol., 46, 7454-7462, 2012.

491 Liu, J., Mauzerall, D. L., Chen, Q., Zhang, Q., Song, Y., Peng, W.; Klimont, Z., Qiu, X., Zhang, S., Hu, M., Lin, W.,

492   Smith, K.R., and Zhu, T.: Air pollutant emissions from Chinese households: A major and underappreciated

493   ambient pollution source, Proc. Natl. Acad. Sci. USA, 113, 28, 7756-7761, 2016.

494 Marotta, A., Pavlovic J., Ciuffo, B., Serra, S., Fontaras, G: Gaseous Emissions from Light-Duty Vehicles: Moving from

495   NEDC to the New WLTP Test Procedure, Environ. Sci. Technol., 49 (14), 8315–8322, 2015.

496 Ministry of Environment Protection of China.: Technical guide for the compilation of emission inventory for

497   atmospheric fine particulates, 2014 (in Chinese).

498 Nguyen, Q.T., Kristensen, T.B., Hansen, A.M.K., Skov, H., Bossi, R., Massling, A., Sørensen, L.L., Bilde, M., Glasius,

499   M., Nøjgaard, J.K.: Characterization of humic-like substances in Arctic aerosols, J. Geophys. Res., 119, 5011-5027,

500   2014.

501 Park, S. S. and Yu, J.: Chemical and light absorption properties of humic-like substances from biomass burning

502   emissions under controlled combustion experiments, Atmos. Environ., 136, 114-122, 2016.

503 Park, S.S., Cho, S.Y., and Bae, M.S.: Source identification of water-soluble organic aerosols at a roadway site using a

504   positive matrix factorization analysis, Sci. Total Environ., 533, 410-421, 2015.

505 Park, S.S., Cho, S.Y., Kim, K.W., Lee, K.H., and Jung, K.: Investigation of organic aerosol sources using fractionated

506   water-soluble organic carbon measured at an urban site. Atmos. Environ., 55, 64-72, 2012.

507 Pavlovic, J. and Hopke, P.K.: Chemical nature and molecular weight distribution of the water-soluble fine and ultrafine

508   PM fractions collected in a rural environment, Atmos. Environ., 59, 264-271, 2012.

509 Pio, C.A., Legrand, M., Alves, C.V., Oliveira, T., Afonso, J., Caseiro, A., Puxbaum, H., Sanchez-Ochoa, A., and

510   Gelencsér, A.: Chemical composition of atmospheric aerosols during the 2003 summer intense forest fire period,

511   Atmos. Environ., 42, 7530-7543, 2008.

512 Riva, M., Healy, R.M., Flaud, P.-M., Perraudin, E., Wenger, J.C., Villenave, E.: Gas- and Particle-Phase Products from

513   the Chlorine-Initiated Oxidation of Polycyclic Aromatic Hydrocarbons, The Journal of Physical Chemistry A 119,

514   11170-11181, 2015.

515 Salma, I., Mészáros, T., and Maenhaut, W.: Mass size distribution of carbon in atmospheric humic-like substances and

516   water soluble organic carbon for an urban environment, J. Aerosol Sci., 56, 53-60, 2013.

517   Salma, I., Mészáros, T., Maenhaut, W., Vass, E., and Majer, Z.: Chirality and the origin of atmospheric humic-like

518   substances, Atmos. Chem. Phys., 10, 1315-1327, 2010.

519   Salma, I., Ocskay, R., and Láng, GG: Properties of atmospheric humic-like substances – water system, Atmos. Chem.

520   Phys., 8, 2243-2254, 2008.

521   Salma, I., Ocskay, R., Chi, X.G, and Maenhaut, W.: Sampling artefacts, concentration and chemical composition of fine

522   water-soluble organic carbon and humic-like substances in a continental urban atmospheric environment, Atmos.

523   Environ., 41, 4106-4118, 2007.

524   Schmidl, C., Bauer, H., Dattler, A., Hitzenberger, R., Weissenboeck, G, Marr, I. L., and Puxbaum, H.: Chemical

525   characterisation of particle emissions from burning leaves, Atmos. Environ., 42, 9070–9079, 2008.

526   Schmidl, C., Marr, L. L., Caseiro, A., Kotianova, P., Berner, A., Bauer, H., Kasper-Giebl, A., and Puxbaum, H.

527   Chemical characterisation of fine particle emissions from wood stove combustion of common woods growing in

528   mid-European Alpine regions, Atmos. Environ., 42, 126–141, 2008.

529   Shen, Z.X., Cao, J.J., Arimoto, R., Han, Z.W., Zhang, R.J., Han, Y.M., Liu, S.X., Okuda, T., Nakao, S., and Tanaka, S.:

530   Ionic composition of TSP and PM$_{2.5}$ during dust storms and air pollution episodes at Xi'an, China, Atmos.

531   Environ., 43, 2911-2918, 2009.

532   Song, J.Z., He, L.L., Peng, P.A., Zhao, J.P., and Ma, S.X. Chemical and isotopic composition of humic-like substances

533   (HULIS) in ambient aerosols in Guangzhou, South China, Aerosol Sci. Technol., 46, 533-546, 2012.

534   Srivastava, D., Tomaz, S., Favez, O., Lanzafame, G M., Golly, B., Besombes, J.-L., Alleman, L. Y., Jaffrezo, J.-L.,

535   Jacob, V., Perraudin, E., Villenave E., and Albinet, A.: Speciation of organic fraction does matter for source

536   apportionment. Part 1: A one-year campaign in Grenoble (France), Sci. Total Environ., 624, 1598–1611, 2018.

537   Tan, J., Xiang, P., Zhou, X., Duan, J., Ma, Y., He, K., Cheng, Y, Yu, J., and Querol, X.: Chemical characterization of

538   humic-like substances (HULIS) in PM$_{2.5}$ in Lanzhou, China. Sci. Total Environ., 573, 1481-1490, 2016.

539   Turpin, B. J. and Huntzicker, J. J.: Identification of Secondary Organic Aerosol Episodes and Quantitation of Primary

540   and Secondary Organic Aerosol Concentrations during Scaqs., Atmos. Environ., 29, 3527–3544, 1995.

541   Varga, B., Kiss, G, Ganszky, I., Gelencser, A., and Krivacsy, Z.: Isolation of water-soluble organic matter from

542   atmospheric aerosol, Talanta, 55, 561–572, 2001.

543   Verma, V., Rico-Martinez, R., Kotra, N., King, L., Liu, J. M., Snell, T. W., and Weber, R. J.: Contribution of

544   Water-Soluble and In-soluble Components and Their Hydrophobic/Hydrophilic Sub-fractions to the Reactive

545   Oxygen Species-Generating Potential of Fine Ambient Aerosols, Environ. Sci. Technol., 46, 11384–11392, 2012.

546   Voliotis, A., Prokes R., Lammel, G, and Samara C. New insights on humic-like substances associated with wintertime

547   urban aerosols from central and southern Europe: Size-resolved chemical characterization and optical properties,

548   Atmos. Environ., 166, 286-299, 2017.

549 Wang, B. and Knopf D. A.: Heterogeneous ice nucleation on particles composed of humic-like substances impacted by

550   O₃, J. Geophys. Res., 116, D03205, doi:10.1029/2010JD014964, 2011.

551 Wang, D. S., Liu, M. R., Bai, X. F., and Ding, H.: The situation analysis of civil coal in the Beijing-Tianjin-Hebei

552   Region, Technology of Coal, 3, 47-50, 2016 (in Chinese).

553 Wang, D.S., Ruiz, L.H.: Secondary organic aerosol from chlorine-initiated oxidation of isoprene, Atmos. Chem. Phys.

554   17, 13491-13508, 2015.

555 Wang, H., Tian, M., Li, X., Chang, Q., Cao, J., Yang, F., Ma, Y., and He, K.: Chemical Composition and Light

556   Extinction Contribution of PM₂.₅ in Urban Beijing for a 1-Year Period, Aerosol Air Qual. Res., 15, 2200–2211,

557   2015.

558 Wang, Y, Hopke, P.K., Rattigan, O.V., Chalupa, D.C., and Utell, M.J.: Source apportionment of airborne particulate

559   matter using inorganic and organic species as tracers, Atmos. Environ., 55, 525–532, 2012.

560 Wang, Y, Hopke, P.K., Rattigan, O.V., Xia, X., Chalupa, D.C., and Utell, M.J.: Characterization of residential wood

561   combustion particles using the two-wavelength aethalometer, Environ Sci. Technol., 45, 7387–7393, 2011.

562 Wiedinmyer, C., Akagi, S.K., Yokelson, R.J., Emmons, L.K., Al-Saadi, J.A., Orlando, J.J., and Soja, A.J.: The Fire

563   INventory from NCAR (FINN): a high resolution global model to estimate the emissions from open burning,

564   Geosci. Model Dev., 4, 625-641, 2011.

565 Yao, X., Chan, C. K., Fang, M., Cadle, S., Chan, T., Mulawac, P., He K., and Ye, B.: The water-soluble ionic

566   composition of PM₂.₅ in Shanghai and Beijing, China, Atmos. Environ., 36, 4223–4234, 2002.

567 Ying, Q., Feng, M., Song, D., Wu, L., Hu, J., Zhang, H., Kleeman, M.J., and Li, X.: Improve regional distribution and

568   source apportionment of PM2.5 trace elements in China using inventory-observation constrained emission factors,

569   Sci. Total Environ., 624, 355-365, 2018.

570 Yu, L., Wang, G, Zhang, R., Zhang, L., Song, Y., Wu, B., Li, X., An, K., and Chu, J.: Characterization and source

571   apportionment of PM₂.₅ in an urban environment in Beijing, Aerosol Air Qual. Res., 13, 574-583, 2013.

572 Zhang, R., Jing, J., Tao, J., Hsu, S. C., Wang, G, Cao, J., Lee, C. S. L., Zhu, L., Chen, Z., Zhao, Y., and Shen, Z.:

573   Chemical characterization and source apportionment of PM₂.₅ in Beijing: seasonal perspective, Atmos. Chem.

574   Phys., 13, 7053-7074, 2013.

575 Zhao, M.F., Huang, Z.S., Qiao, T., Zhang, Y.K., Xiu, GL., and Yu, J.Z.: Chemical characterization, the transport

576   pathways and potential sources of PM2.5 in Shanghai: Seasonal variations, Atmos. Res., 158-159, 66-78, 2015.

577   Zheng, G J., Duan, F.K., Su, H., Ma, Y.L., Cheng, Y., Zheng, B., Zhang, Q., Huang, T., Kimoto, T., Chang, D., Pöschl,

578   U., Cheng, Y. F., and He, K. B.: Exploring the severe winter haze in Beijing: the impact of synoptic weather,

579   regional transport and heterogeneous reactions, Atmos. Chem. Phys., 15, 2969-2983, 2015.
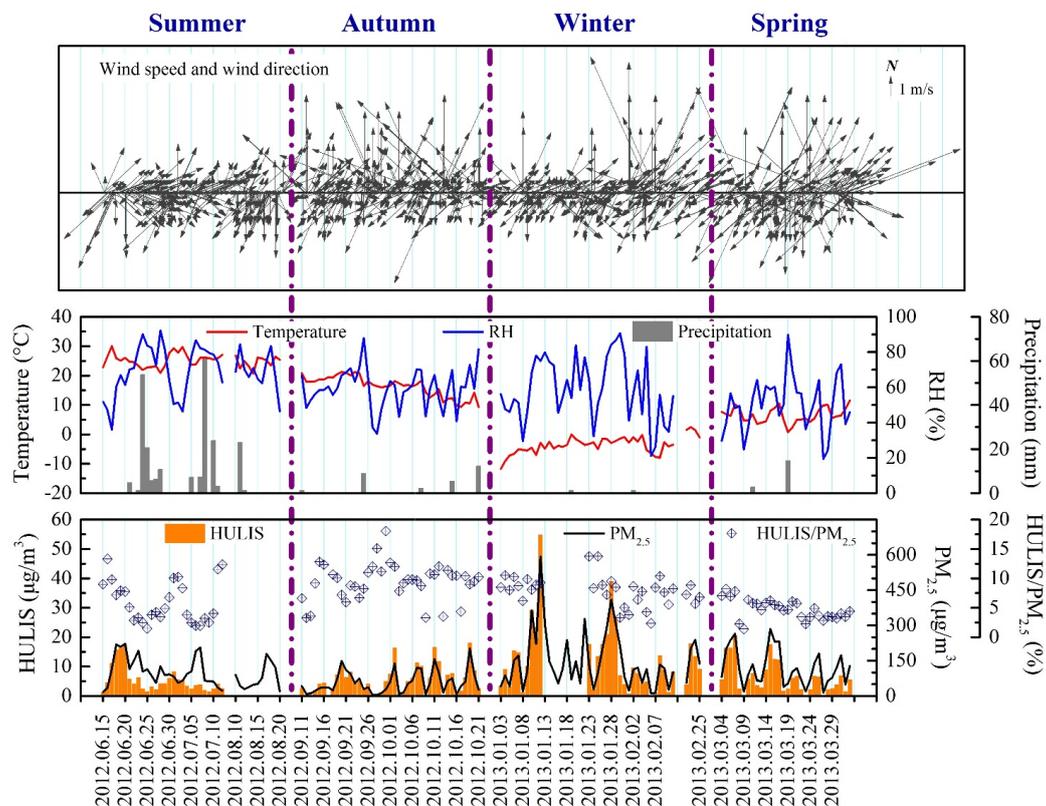
580   Zheng, G J., He, K.B., Duan, F.K., Cheng, Y., and Ma, Y. L.: Measurement of humic-like substances in aerosols: A

581   review, Environ. Pollut., 181, 301-314, 2013.

582

583

584 **Figures**

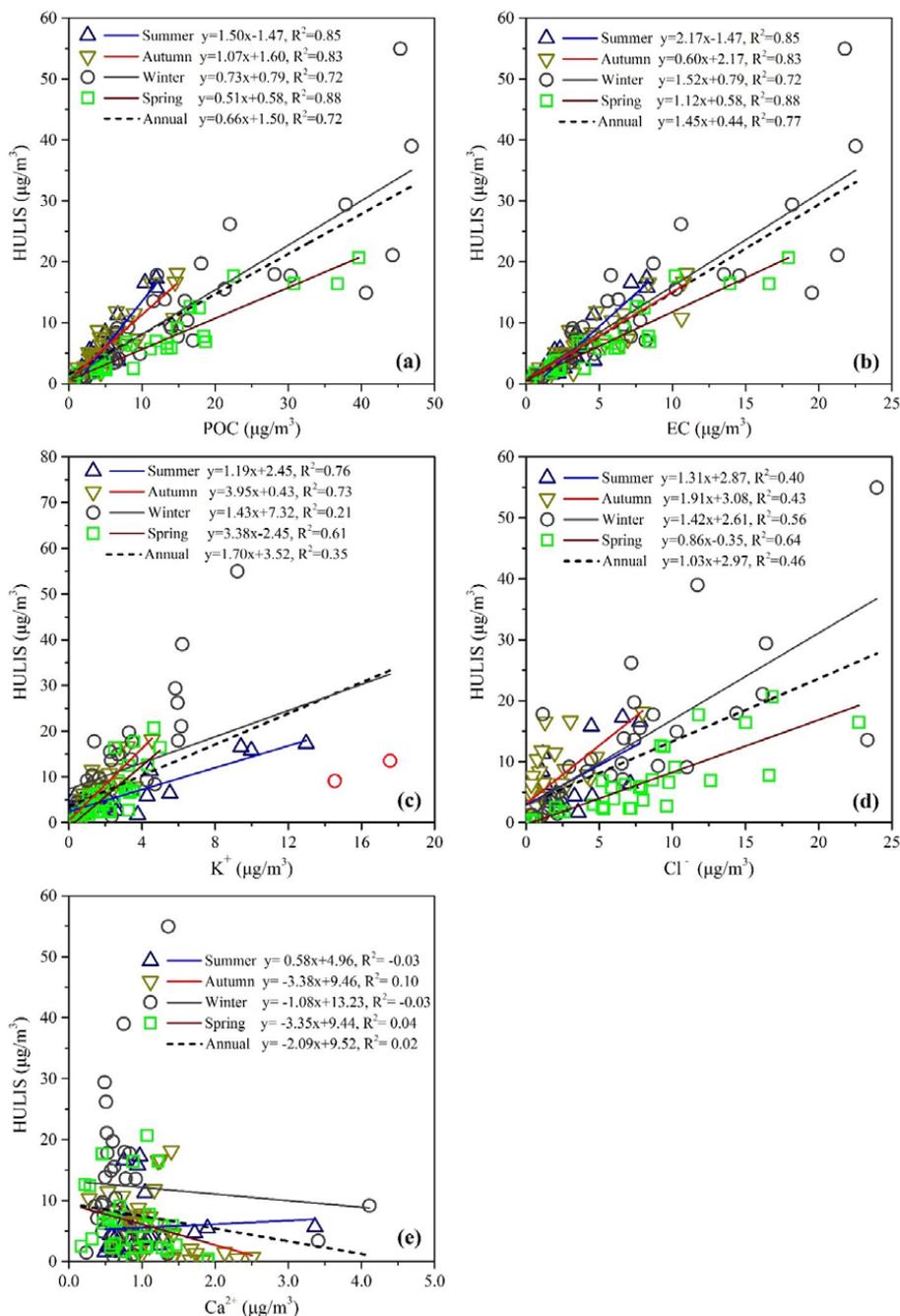586 **Figure 1.** Time series of meteorological data (wind speed, wind direction, temperature, relative humidity and

587 precipitation), HULIS, PM$_{2.5}$ and HULIS/PM$_{2.5}$ for the sampling period.

585

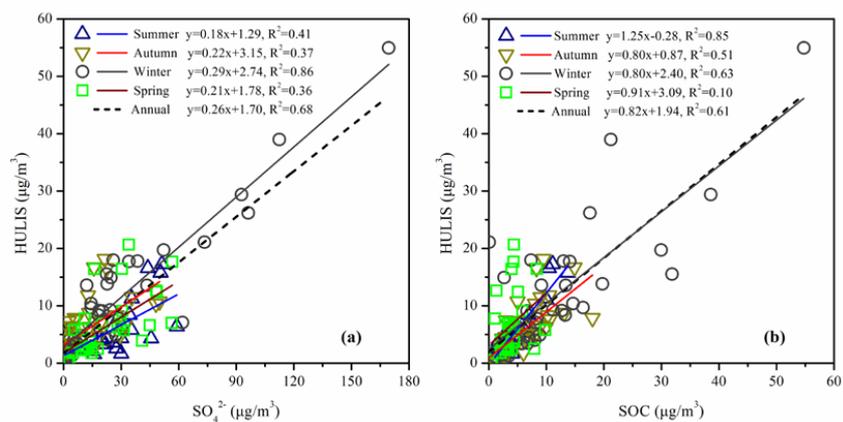588

589

Atmospheric
Chemistry
and Physics
Discussions

590

591

Figure 2. Correlations between HULIS and POC (a), HULIS & EC (b), HULIS & K⁺(c), HULIS & Cl⁻(d), HULIS &

593   Ca²⁺(e). Concentrations in four seasons are represented by different shaped points with different colors. Linear

594   regressions are also given with corresponding equations.

595

596

Figure 3. Correlations between HULIS & SO_4^{2-} (a), HULIS and SOC (b). Concentrations in four seasons are
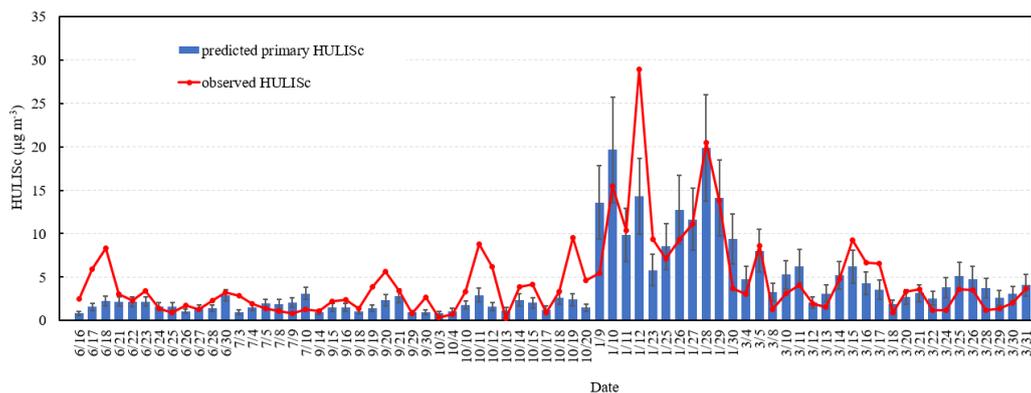
represented by different shaped points with different colors. Linear regressions are also given with corresponding

equations.

600

601

602

Figure 4. Predicted primary HULISc and observed HULISc concentrations on the days with relatively good primary

PM$_{2.5}$ model performance. Error bar is the standard deviation of prediction, which is calculated as described in SI Text

S3.1.

606

607

608

Figure 5. Scatter plot of predicted primary HULISc and observed HULISc concentrations. Concentrations of each

seasons are represented by different shaped points with different colors. Linear regressions are also given with
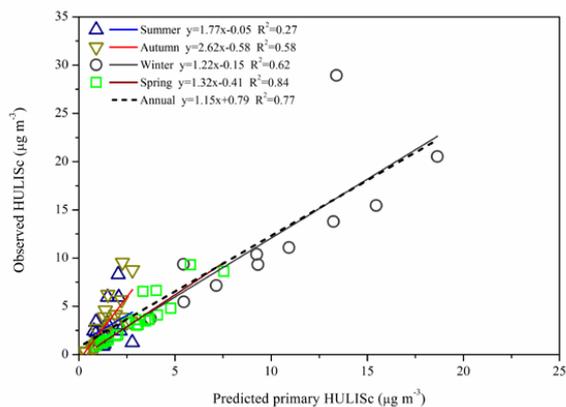
corresponding equations.

612

613 **Tables**

614 **Table 1.** Summary of the concentrations of PM$_{2.5}$, carbon species, water-soluble ions and percentages of several species

615 to some others.

Species	Average	Summer	Autumn	Winter	Spring
	Average ± SD	Average ± SD	Average ± SD	Average ± SD	Average ± SD
PM$_{2.5}$ (μg/m^3)	106±89	98 ± 60	58±48	150±121	120±76
OC (μg/m^3)	16.0±15.8	8.5±5.2	10.3±7.4	28.9±22.0	14.6±10.8
EC (μg/m^3)	5.0±4.8	3.3±1.8	3.5±2.9	7.8±6.6	5.3±4.7
OC/EC	3.6±1.4	2.8±0.8	3.8±1.9	4.3±1.2	3.3±0.9
WSOC (μg/m^3)	6.5±6.5	4.4±3.6	5.2±4.0	10.3±9.8	5.9±4.9
HULIS (μg/m^3)	7.5±7.8	5.5±4.4	5.6±4.7	12.3±11.7	6.5±5.5
HULIS/PM$_{2.5}$ (%)	7.2±3.3	5.9±3.5	9.4±3.1	7.9±2.5	4.8±1.7
HULIS$_C$/OC (%)	24.5±8.3	29.2±6.2	26.2±9.6	21.0±7.1	22.0±6.9
HULIS$_C$/WSOC (%)	59.5±9.2	66.7±5.4	54.1±11.2	62.3±5.7	56.6±6.3
SO$_4^{2-}$ (μg/m^3)	22.3±24.1	22.6±17.0	10.9±13.2	32.7±35.1	22.5±16.5
NO$_3^-$ (μg/m^3)	18.6±18.0	17.2±13.4	10.8±13.2	20.1±17.8	29.0±23.8
Cl$^-$ (μg/m^3)	4.2±4.9	1.8±1.9	1.3±1.6	6.5±5.7	7.9±5.2
Na$^+$ (μg/m^3)	0.60±0.51	0.40±0.30	0.33±0.41	0.89±0.61	0.79±0.36
K$^+$ (μg/m^3)	2.2±2.6	2.2±2.9	1.3±1.0	3.2±3.6	2.2±1.3
Mg^{2+} (μg/m^3)	0.18±0.19	0.15±0.07	0.18±0.08	0.24±0.32	0.10±0.07
Ca^{2+} (μg/m^3)	0.97±0.57	0.99±0.52	1.14±0.48	0.83±0.70	0.89±0.46
NH$_4^+$ (μg/m^3)	14.1±13.0	13.2±9.8	6.6±7.0	19.1±16.9	18.4±11.8

616

617

618   **Table 2.** $HULIS_C/OC$ and $HULIS_C/WSOC$ values in the source samples

Source type	Stove/vehicle	$HULIS_C/OC$	$HULIS_C/WSOC$	n
Residential biofuel burning				
wood burning	improve stove	0.41±0.07	0.62±0.06	3
wheat straw	improve stove	0.50±0.04	0.65±0.05	4
corn stover	improve stove	0.42±0.04	0.62±0.04	3
Residential chunk coal combustion				
SM, Var=32.4%	high efficiency heating stove	0.14±0.07	0.51±0.04	3
JY, Var=27.7%	high efficiency heating stove	0.18±0.04	0.50±0.04	3
BH, Var=25.0%	high efficiency heating stove	0.08±0.02	0.44±0.01	3
DT, Var=19.4%	high efficiency heating stove	0.15	0.62	1
SM, Var=32.4%	traditional cooking and heating stove	0.06±0.01	0.46±0.02	3
JY, Var=27.7%	traditional cooking and heating stove	0.07±0.03	0.41±0.06	3
BH, Var=25.0%	traditional cooking and heating stove	0.05±0.01	0.43±0.08	3
Residential briquette coal combustion				
XM, Var=9.6%	high efficiency heating stove	0.24±0.07	0.53±0.09	3
Vehicle exhaust				
traffic tunnel	mixed of gasoline and diesel vehicles	0.05	0.65	1
heavy-duty diesel trucks	Euro II	0.16±0.02	0.38±0.03	3
light-duty gasoline vehicles	Euro IV	0.11±0.03	0.21±0.11	4

619

620

621   **Table 3.** Average and seasonal contributions percent of various sources to ambient HULIS concentrations in Beijing

622   (%)

	Residential biofuel burning	Residential coal burning	Transportation	Industries	Biomass open burning	Secondary process
Average	57.4±9.1	12.3±2.8	1.5±0.3	1.1±0.3	1.7±0.5	25.9±9.3
Summer	36.3±8.7	7.8±2.6	2.9±0.9	2.4±1.2	10.3±3.5	40.2±18.1
Autumn	34.7±8.2	7.4±2.3	2.3±0.7	1.6±0.8	1.3±0.7	52.7±17.1
Winter	69.6±20.2	14.9±6.1	0.8±0.3	0.5±0.3	0.0±0.0	14.3±18.2
Spring	69.7±17.0	14.9±5.1	1.3±0.4	0.9±0.4	0.1±0.0	13.1±13.4

623   Note: only the sources with an average contribution over than 1% were provided. Uncertainty estimation for the

624   seasonal and annual primary and secondary HULISc contributions was determined using a bootstrap sampling

625   technique, which is described in Text S3.2. These uncertainties are based on the assumption that the uncertainty of the

626   PPM$_{2.5}$ and f$_{OC}$ values are 30% and 15%, respectively. Uncertainty calculations based on larger uncertainties (50% for

627   both PPM$_{2.5}$ and f$_{OC}$) show 5-10% higher relative uncertainties for the residential biofuel and secondary process but

628   small changes for other primary sectors (see Table S5).